Architecture, antenatal activity and arrhythmia of the human foetal heart:
A Computational Database

Eleftheria Pervolaraki[1], Richard A Anderson[2], Alan P Benson[1], Barrie Hayes-Gill[3], Arun V Holden[1], Benjamin Moore[1], Henggui Zhang[4]

[1]Institute of Membrane and Systems Biology, University of Leeds, Leeds LS2 9JT, UK; [2]MRC Centre for Reproductive Health, University of Edinburgh, Edinburgh EH16 4T3; [3]Electrical and Electronic Engineering, University of Nottingham, Nottingham NG7 2RD, UK; Physics and Astronomy, University of Manchester, Manchester M13 9PL

Correspondence: a.v.holden@leeds.ac.uk

Background. The computational biology of the electrodynamics of the heart [1] is largely based on models and data sets from laboratory animals. A computational model of the heart facilitates the interpretation of noninvasive, high resolution, multichannel recordings [2] from an individual, and requires datasets of cardiac geometry, anisotropy and electro-physiology.

Aim. This project will deliver ~100µm resolution models of human foetal heart geometry and anisotropy at different gestational ages, and sub-ms resolution models of ventricular electrophysiology informed by foetal ECG characteristics. These are applied to evaluate the hypothesis that late miscarriage and stillbirth, in the 60% of cases where there is no obvious cause, may be due to re-entrant arrhythmia in the foetal heart.

Methods. Human foetal hearts (age range 14-17 weeks) were obtained from abortions that may be performed until the 24th week of pregnancy (see Figure 1).

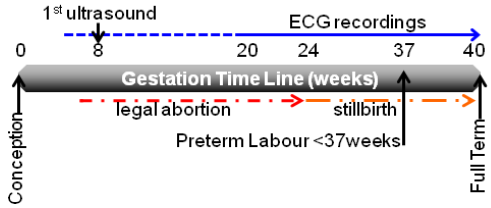

Fig.1 An illustration of the gestational time line representing important stages from conception to birth.

The 3D structure of the heart can be reconstructed non-invasively by Magnetic Resonance Imaging (MRI) or micro-computed tomography (µCT), and any anisotropic architecture by diffusion tensor MRI. Fibre orientation can be estimated from high-resolution µCT. Hearts in fomblin were imaged on a 9.4T Bruker BioSpin: 15ms echo time, 500ms repetition time and a b value of 1000s/mm^2. Each slice was 1mm with a 1mm gap between the slices. In each scan, diffusion-weighted images were obtained in 12 directions. µCT imaging, using the Nikon Metris 225/320 at the Henry Moseley Imaging Centre, Manchester used iodine (Lugol solution) as a contrast agent [3]. All 3D visualisations were performed in VolView (www.kitware.com).

Foetal electrocardiogram (fECG) was recorded through a 5-electrode high-sensitivity device on the maternal abdomen (from one volunteer, from 20 to 40 weeks) using Monica AN24 (Monica Healthcare Ltd) during maternal rest and activity, and ECG intervals (PR, QR, RS, QS) that relate to propagation times, and QT, and its dispersion, that relate to ventricular action potential durations, extracted. Foetal QT and RR intervals, and ventricular cell action potential durations (APD) were extracted from the literature [4, 5], and computed using the ten Tusscher-Panfilov model [6].

Results. The surfaces and 3D computational grid of 3 foetal hearts are illustrated in Figures 2 and 3 and their anisotropic architecture is represented in Figures 4, 5 and 6. Coronary arteries are visible on the surface, and the left atrial appendage is developing as a cochloid. The computational grids have a spatial resolution of 100×100×100 to 179×179×179 µm, which allows interpolation to an isotropic grid suitable for numerical solution of the excitation equations [7] for human tissue.

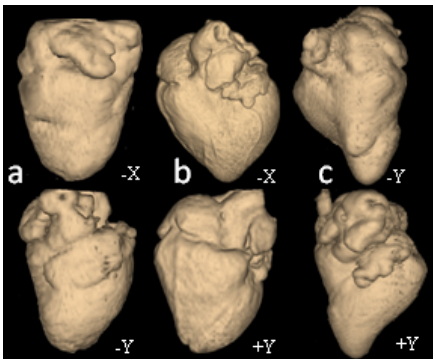

Fig.2 3D surface diffusion weighted images of three human foetal hearts, (a) at 14+4/7 (b) 15 +5/7 (c) 16 +4/7 weeks gestational age.

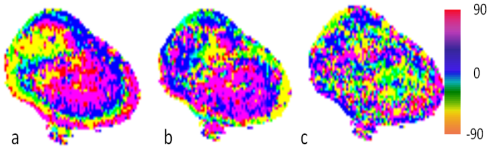

Fig.4 Visualisation of angles that define tissue architecture for short axis ventricular slice of 15+5/7 heart (a) helix angle and (b) transverse angle of primary eigenvector; (c) normal to tertiary eigenvector ("sheet").

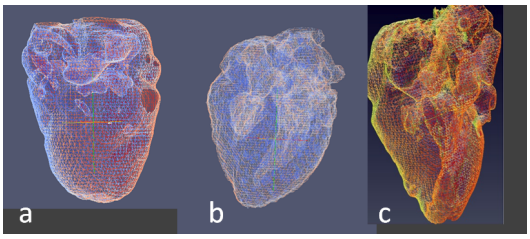

Fig.3 3D computational grids for the three foetal hearts. (a) 14+ 4/7 (b) 15+5/7 (c) 16 +4/7 weeks gestational age.

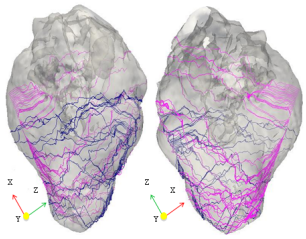

Fig.5 Tracking of "streamlines" of the orientation of the estimated primary eigenvector field ("fibre orientation") from ventricular endocardial seed points in; 16 +4/7 week foetal heart illustrates gross helical organisation of the primary eigenvector, the "fibre orientation" [8].

The smooth 120˚ change in the helix angle of the primary eigenvector ("myofibre" helix angle), from positive to negative, that is seen in mammalian hearts, including the full term and adult human heart and >40 days gestational age pig foetal heart is present if the transmural angles are averaged within ventricular wall segments, but is not clear at the voxel level. The helix and transverse angles appear more irregular, but tracking the streamlines in the primary eigenvector field ("fibre tracking", Figure 5) shows the gross helical organisation of the myocardial architecture.

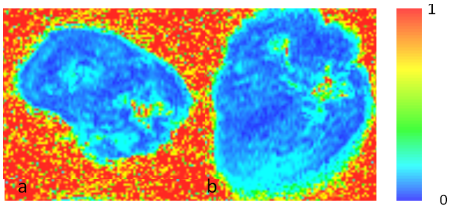

Fig.6 Fractional anisotropy of (a) short and (b) long axis slice through foetal myocardium of 15+5/7 week gestational age heart.

The three foetal hearts all show a low (mean ~0.2) fractional anisotropy, and so the irregularity in angle spatial distribution can be related to the primary eigenvalues being greater, but not very much greater than the secondary and tertiary eigenvalues. Quantitative histology can relate this to either a not very elongated myocardial cell shape, or poorly developed compactification of the mid- and sub-endocardium. The fECG can be extracted from high sensitivity recordings on the maternal abdominal surface, and the fECG intervals extracted. The morphology of a sample average fECG is shown in Figure 8. The PR and QR intervals are indices of propagation times, while the QT interval is an index of ventricular action potential duration. The foetal QT intervals and cell APD can be approximated by an unmodified human epicardial [6] model. The PR intervals do not change systematically after 25 weeks during gestation and the QR intervals decrease (Figure 9): this is while there is a two-fold increase in the linear dimensions of the heart. This implies a more than two- fold increase in conduction velocity, which is of the order of 10cm/s. For an APD of 200ms the wavelength of a re-entrant wave would be ~ 2cm, and so a re-entrant is possible.

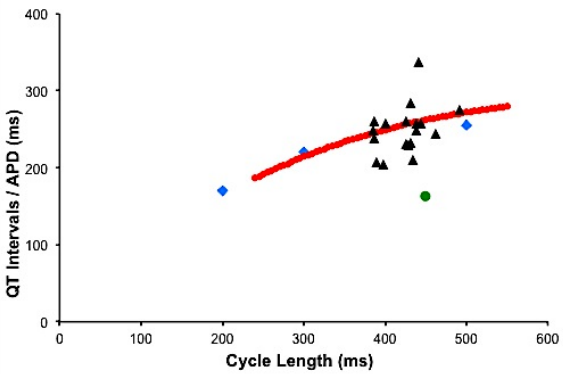

Fig.7 ● computed periodic APD_{90} for human ventricular cell model [6], ▲ foetal QT intervals ♦ foetal APD_{60} from [5], ● is the fECG cycle illustrated in Figure 8.

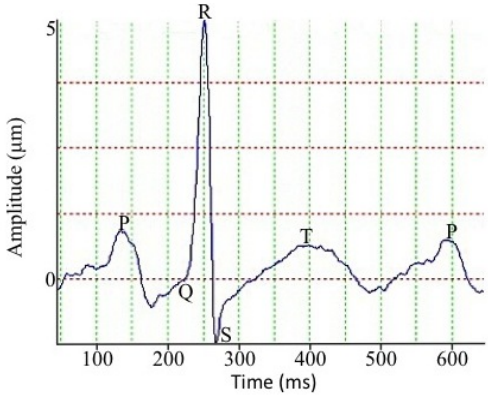

Fig.8 Averaged cycle of foetal ECG (fECG) produced by Monica AN24 from one pregnant volunteer, with P, Q, R, S, T wave times indicated. This cycle is also represented as the green point in Figure 7.

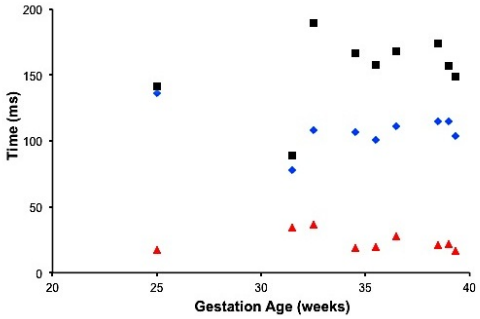

Fig.9 Representation of foetal QT ■, PR ♦ and QR ▲ intervals as measured using the Monica AN24 from one pregnant volunteer at rest, throughout gestation.

The human foetal heart data structure and architecture datasets are available as processed files (intensity, trace, fractional anisotropy, helix angles, transverse angles of primary eigenvectors, "sheet" normal to tertiary eigenvectors) and as their separate components in the form of ".vtk" files. See WWW.VTEA.LEEDS.AC.UK for further details (the archive is still under construction and is due to be online from September 2012).

References.

1. Vadakkumpadan F, Arevalo H, Prassl AJ, Chen J, Kickinger F, Kohl P, Plank G, Trayanova N, 2010, Image-based models of cardiac structure in health and disease. *Syst Biol Med* 2:489-506.

2. Rudy Y, 2009, Noninvasive imaging of cardiac electrophysiology and arrhythmia. *Ann NY Acad Sci* 1188:214-221.

3. Aslanidi OV *et al.* 2012, Application of X-ray Micro-Computed tomography with iodine staining to cardiac imaging, segmentation and model development. Submitted to *IEEE BME*.

4. Aboud S, Barkal G, Mashiachi S, Sadeh H, 1990, Quantification of the fetal ECG using averaging technique. *Comput Biol Med* 20(3):147-155.

5. Jekez K, Pucelik J, Sauer J, Bartak F, 1982, Basic electrophysiological parameters and frequency sensitivity of the ventricular myocardium of human embryos. *Physiologia Bohemoslvaca* 31(1):11-19.

6. Ten Tusscher KH, Noble D, Noble PJ & Panfilov AV, 2004, A model for human ventricular tissue. *Am J Physiol* 286(4):H1573-H1589.

7. Benson AP, Bernus O, Dierckx H, Gilbert SH, Greenwood JP, Holden AV, Mohee K, Plein S, Radjenovic A, Ries ME, Smith GL, Sourbron S, Walton RD, 2011, Construction and validation of anisotropic and orthotropic ventricular geometries for quantitative predictive cardiac electrophysiology. *Interface Focus* 1(1):101-116.

8. Gilbert SH, Benson AP, Li P & Holden AV, 2007, Regional localisation of left ventricular sheet structure: integration with current models of cardiac fibre, sheet and band structure. *Eur J Cardiothorac Surg* 32(2):231-249.